Stagnation-Point Flow and Heat Transfer Towards a Shrinking Sheet with Suction in an Upper Convected Maxwell Fluid

Yian Yian Lok[a], Anuar Ishak[b], and Ioan Pop[c]

[a] Mathematics Section, School of Distance Education, Universiti Sains Malaysia, 11800 USM, Pulau Pinang, Malaysia
[b] School of Mathematical Sciences, Faculty of Science and Technology, Universiti Kebangsaan Malaysia, 43600 UKM Bangi, Malaysia
[c] Department of Mathematics, Babeş-Bolyai University, R-400048 Cluj-Napoca, Romania

Reprint requests to I. P.; E-mail: popm.ioan@yahoo.co.uk

Z. Naturforsch. **68a,** 693 – 700 (2013) / DOI: 10.5560/ZNA.2013-0047
Received October 21, 2012 / revised June 25, 2013 / published online August 21, 2013

A steady two-dimensional boundary-layer flow and heat transfer of an upper convected Maxwell fluid near a stagnation-point of a permeable shrinking sheet is studied numerically. The effects of elasticity, shrinking, and suction parameters on the flow and heat transfer characteristics are investigated. A similarity transformation reduces the governing equations to third-order nonlinear ordinary differential equations which are then solved numerically. For a fixed value of elastic parameter, it is found that dual solutions exist for some values of shrinking and suction parameters. The plotted streamlines show that for upper branch solutions, the effects of shrinking and suction are direct and obvious as the flow near the surface is seen to suck through the permeable sheet and drag to the origin of the sheet. However, aligned but reverse flow occurs for the case of lower branch solutions.

Key words: Stagnation-Point Flow; Shrinking Sheet; Maxwell Fluid; Boundary Layer; Suction.

1. Introduction

Some industrial fluids such as polymeric fluids, slurries, lubrication oils and greases, are capable of flowing but demonstrate flow and heat transfer characteristics which cannot be adequately described by the classical Newtonian model. These fluids are named as viscoelastic fluids, i. e. fluids which exhibit both viscous and elastic characteristics that enable the fluids keep memory of their past deformations. Many models have been suggested to describe the behaviours of the viscoelastic fluids; one of them is the upper convected Maxwell (UCM) fluid which takes into account the stress relaxation that exists in the flow. There are quite a number of studies on UCM fluids, however, not many papers that deal with stagnation-point flow published in open literature. In the history of fluid dynamics, the study of stagnation-point flow in different type of fluid medium has always become the focus interest of many researchers. Although the stagnation-point flow solution is valid in a small region in the vicinity of the stagnation-point, it represents flow with engineering significance and the stagnation-point solution may serve as a starting solution for the solution over the entire body.

The plane and axisymmetric stagnation flow of a Maxwell fluid has been studied by Phan-Thien [1]. Exact solutions, including inertia, to the above problem have been reported in that paper. Hayat et al. [2] and Abbas et al. [3] solved the stagnation-point flow of an UCM fluid over a stretching surface in the presence of constant magnetic field and buoyancy force, respectively, using the homotopy analysis method (HAM). In addition, Abbas et al. [3] have also solved the problem numerically using a finite difference method and then compared the results with the analytical solution by HAM. Recently, Hayat et al. [4] used the HAM to study the influence of melting heat transfer on stagnation-point flow of UCM fluid towards a stretching sheet. They found that the local Nusselt number is a decreasing function of the melting parameter. Also, Nadeem et al. [5] used HAM to solve the problem of stagnation flow of a Maxwell fluid over a shrinking sheet. All these four papers [2 – 5]

found that elasticity decreases the boundary layer thickness.

On the other hand, Sadeghy et al. [6] presented the theory and results for two-dimensional boundary layer stagnation-point flow of UCM fluids while Kumari and Nath [7] studied the steady state magnetohydrodynamic (MHD) mixed convection flow of UCM fluids near the stagnation-point. They found that there is no velocity overshoot in the UCM model as found by Beard and Walters [8] in second-grade fluids. Besides, thickening of boundary layer and decreasing in reduced skin friction coefficient $f''(0)$ is predicted to exist for the high elasticity number of the UCM model. This prediction is controversial to those reported for the Maxwell model used by Phan-Thien [1], Hayat et al. [2, 4], Abbas et al. [3], and Nadeem et al. [5]. It is further found that the papers by Sadeghy et al. [6] and Kumari and Nath [7] considered different sign of elasticity term as used in Hayat et al. [2, 4], Abbas et al. [3], and Nadeem et al. [5]. It has to be mentioned here that the controversial and confusion over viscoelastic model, specifically flow retardation, and model approximation of the second-grade model has been discussed in detail by Dunn and Rajagopal [9]. Also, Garg and Rajagopal [10] pointed out that the sign adopted by Beard and Walters [8] and many other authors for the elastic term should be reversed to comply with thermodynamic constrain. We mention to this end, that very recently Rajagopal [11] has generalized the classical viscoelastic fluid model due to Maxwell to allow the relaxation time and the viscosity to depend on the stress.

Recently, the flow due to a stretching sheet has been studied rigorously because of its important applications in industries such as manufacturing of polymer sheets, filaments, and wires. During the manufacturing process, the moving sheet is assumed to stretch on its own plane and the stretched surface interacts with the ambient fluid both mechanically and thermally. More recently, the boundary layer flow due to a shrinking sheet has gained considerable interest. In contrast to a stretching sheet, for the shrinking case, the sheet is shrunk towards a fixed point which would cause a velocity away from the sheet. This phenomenon can be found, for example, on a rising and shrinking balloon, or a moving and shrinking polymer film. Wang [12] was the first to study the unsteady viscous flow by a shrinking film. The closed form exact solution of the viscous flow with suction has been obtained by Miklavčič and Wang [13] who found that the solutions may not unique for certain suction rates. There are two conditions for shrinking flow to exist physically, i. e. either imposed adequate suction on the boundary (Miklavčič and Wang [13]) or added stagnation flow which contains the vorticity (Wang [14]). Since then, many authors have extended the shrinking problem to other fluid media with the imposition of either suction, stagnation flow or both.

The aim of this study is to investigate the steady two-dimensional stagnation-point flow of an upper convected Maxwell fluid impinging on a permeable shrinking sheet. As far as we are concerned, the problem of suction and shrinking effects in the vicinity of stagnation point over UCM fluid has yet to be solved. The applications of this study can be found in engineering and industry fields, for example, the extrusion of polymer sheet which immersed in a non-Newtonian fluid as cooling liquid. This process adversely affects the flow and heat transfer characteristics. In order to control the flow so that the separation of flow does not occur, we can impose the suction so that the velocity of the fluid can be decreased (Saikrishnan and Roy [15]; Roy and Saikrishnan [16]; Mukhopadhyay and Layek [17]). There are also some other ways to control the flow separation and control the velocity and temperature profiles as well as the skin friction on the interface. Out of many one can mention the recent works by Shadloo et al. [18, 19] where they showed the effect of MHD and micropolar fluids, respectively, in order to control before mentioned flow properties.

In this paper, we follow the UCM model which was used by Sadeghy et al. [6] and Kumari and Nath [7]. After applying the boundary layer approximations and similarity transformation, the resulting nonlinear governing equations are solved numerically for some values of the governing parameters. Representative results for the reduced skin friction or shear stress, reduced heat transfer from the surface of the sheet, velocity, and temperature profiles as well as the streamlines of the stagnation-poinnt flow are presented.

2. Problem Formulation

Consider a steady stagnation-point flow and heat transfer towards a permeable shrinking sheet in a UCM fluid. It is assumed that the velocity of the stretching or the shrinking sheet is $u_w(x) = cx$, while the flow velocity outside the boundary layer (inviscid fluid) is

$u_e(x) = ax$, where a (> 0) and c are constants, with $c > 0$ for a stretching sheet and $c < 0$ for a shrinking sheet. It is also assumed that the constant mass transfer velocity is v_w, with $v_w < 0$ for suction and $v_w > 0$ for injection (withdrawal). Further, it is assumed that the uniform temperature of the sheet is T_w, while that of the ambient fluid is T_∞. Following Sadeghy et al. [6] and Kumari and Nath [7], the continuity and momentum boundary layer equations for the stagnation-point flow of the UCM fluid are given by

$$\frac{\partial u}{\partial x} + \frac{\partial v}{\partial y} = 0, \tag{1}$$

$$\frac{\partial u}{\partial x} + v\frac{\partial u}{\partial y} = u_e\frac{\mathrm{d}u_e}{\mathrm{d}x} + \nu\frac{\partial^2 u}{\partial y^2} + k_0 \cdot \left(u^2\frac{\partial^2 u}{\partial x^2} + v^2\frac{\partial^2 u}{\partial y^2} + 2uv\frac{\partial^2 u}{\partial x \partial y}\right). \tag{2}$$

In addition to these equations, we consider also the energy equation

$$u\frac{\partial T}{\partial x} + v\frac{\partial T}{\partial y} = \alpha\frac{\partial^2 T}{\partial y^2} \tag{3}$$

along with the boundary conditions for the present problem

$$\begin{aligned} &u = u_w(x),\ v = v_w,\ T = T_w \ \text{ at } \ y = 0 \\ &u \to u_e(x),\ T \to T_\infty \ \text{ as } \ y \to \infty\ . \end{aligned} \tag{4}$$

Here u and v are the velocity components along the x- and y-axes, respectively, ν is the kinematic viscosity, k_0 is the relaxation time of the UCM fluid, and α is the thermal diffusivity. We mention that (1) and (2) have also been derived in the paper by Sadeghy et al. [20] for the boundary layer flow of a UCM fluid past a moving surface. This equation generalizes the well-known Sakiadis [21] problem for a viscous (Newtonian) fluid.

In order to solve (1)–(3) with the boundary conditions (4), we consider the following similarity variables:

$$\begin{aligned} &\psi = (\nu a)^{1/2} x f(\eta),\ \eta = \left(\frac{a}{\nu}\right)^{1/2} y, \\ &\theta(\eta) = (T - T_\infty)/(T_w - T_\infty), \end{aligned} \tag{5}$$

where ψ is the stream function defined as $u = \partial\psi/\partial y$ and $v = -\partial\psi/\partial x$, which identically satisfies (1). Thus, we have

$$u = axf'(\eta),\ v = -\sqrt{\nu a} f(\eta), \tag{6}$$

where the prime denotes differentiation with respect to η. Substituting (5) into (2) and (3), we obtain the following nonlinear ordinary differential equations:

$$f''' + ff'' + 1 - f'^2 + K(f^2 f''' - 2ff'f'') = 0, \tag{7}$$

$$\frac{1}{\mathrm{Pr}}\theta'' + f\theta' = 0. \tag{8}$$

The boundary conditions (4) now become

$$\begin{aligned} &f(0) = s,\ f'(0) = \frac{c}{a} = \lambda,\ \theta(0) = 1, \\ &f'(\eta) \to 1,\ \theta(\eta) \to 0 \ \text{ as } \ \eta \to \infty. \end{aligned} \tag{9}$$

Here $K = ak_0$ (≥ 0) is the dimensionless elastic parameter also known as Deborah or Weissenger number (Bird et al. [22]), $\mathrm{Pr} = \nu/\alpha$ is the Prandtl number, $\lambda = c/a$ is the stretching $(\lambda > 0)$ or shrinking $(\lambda < 0)$ parameter, and $s = -v_w/(a\nu)^{1/2}$ is the mass transfer parameter with $s > 0$ for suction and $s < 0$ for injection. For $K = s = \lambda = 0$, (7) reduces to the classical Hiemenz [23] problem.

3. Numerical Methods

Equations (7) and (8) subject to the boundary conditions (9) have been solved numerically using the Keller-box method for some values of the governing parameters, namely elastic parameter K, shrinking parameter λ, suction parameter s, and Prandtl number Pr. The Keller-box method is an implicit finite-difference method with second-order accuracy. This method involves four steps. First, by introducing new dependent variables, the ordinary differential equations (7) and (8) were reduced to a first-order system. Then, the system was expressed in finite difference forms using central difference. Next, the resulting nonlinear algebraic equations were linearized using the Newton linearization before and wrote them in matrix–vector form. Lastly, the linear system was solved by the block-tridiagonal-elimination method which consists of forward sweep and backward sweep. The detailed description of this numerical method can be found in the books by Cebeci and Bradshaw [24] and Cebeci [25]. It has been successfully used by the present authors to solve various boundary-value problems (cf. Lok et al. [26]; Ishak et al. [27, 28]).

Before performing the computation, it is necessary to make an initial guess for the initial profiles across

λ	Wang [14] Integration & shooting method	Kimiaeifar et al. [29] Homotopy Analysis Method, 20th-order	Kimiaeifar et al. [29] 4th-order Runge–Kutta method	Present study Keller-box method
−0.25	1.40224	1.402254441	1.40224078	1.40224
−0.5	1.49567	1.495670686	1.495671	1.49567
−0.75	1.48930	1.489335189	1.48933	1.48930
−1	1.32882	1.32888085	1.328824	1.32882
	0			0.00000
−1.15	1.08223			1.08223
	0.116702			0.11670
−1.2				0.93247
				0.23365
−1.2465				0.58430
	0.55430			0.55428

Table 1. Comparison of initial values $f''(0)$ when $K = s = 0$ for some values of λ.

the boundary layer. The selected initial values can be arbitrary but they must satisfy the boundary conditions (9). Besides, the boundary layer thickness η_∞ needs to be determined in order to achieve the far field boundary conditions asymptotically. The step size $\Delta\eta = 0.005$ was found satisfactory for the numerical values to be mesh independent. Further, the iteration numerical procedures were repeated until the final results satisfied the convergence criterion 10^{-7}. For certain range of the shrinking and suction parameters, two solutions were found to exist by setting two different values of the boundary layer thickness η_∞. Both profiles satisfied the far field boundary conditions asymptotically, but with different shapes. In general, for the first (upper branch) solutions, the boundary layer thickness set was between 3 and 6, while for the second (lower branch) solutions, it was between 12 and 20.

4. Results and Discussion

In order to verify our results, the values of the reduced skin friction or reduced shear stress $f''(0)$ with $K = 0$ (viscous or Newtonian fluid) and $s = 0$ (impermeable surface) have been computed. Table 1 shows the comparison of $f''(0)$ with those obtained by Wang [14] and Kimiaeifar et al. [29]. The results are in very good agreement. The velocity profiles $f'(\eta)$ for $K = 0.3$ in the absence of suction parameter and shrinking effect are plotted in Figure 1 for graphical comparison purpose. The compared profiles are deduced from the velocity profiles published by Beard and Walters [8], Sadeghy et al. [6], and Kumari and Nath [7]. The results are found to be in good agreement with those of Maxwell model considered by Sadeghy et al. [6] and Kumari and Nath [7], but differ significantly with those of the second-grade

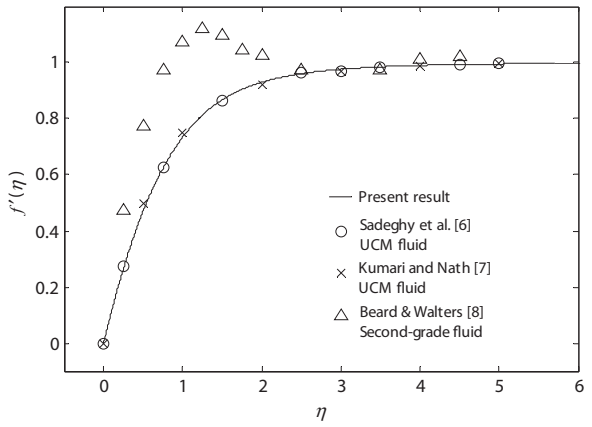

Fig. 1. Comparison of velocity profiles $f'(\eta)$ at $K = 0.3$, $\lambda = s = 0$.

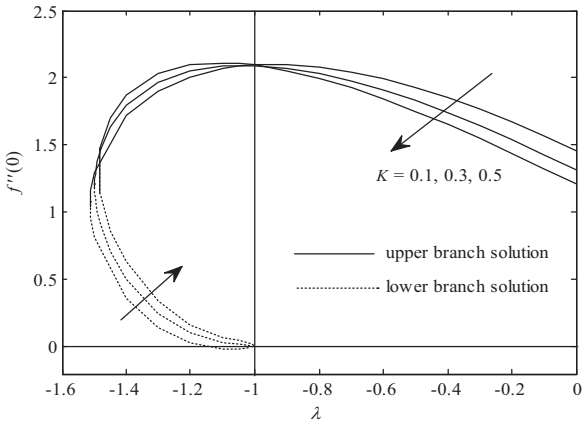

Fig. 2. Variation of $f''(0)$ with the shrinking parameter λ for $s = 0.5$ and some values of K.

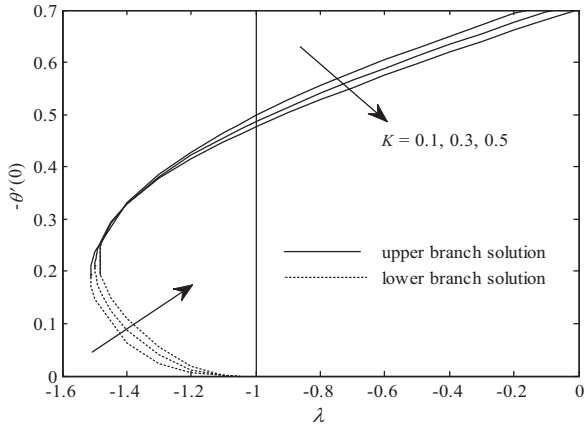

Fig. 3. Variation of $-\theta'(0)$ with the shrinking parameter λ for $s = 0.5$, $\Pr = 0.7$, and some values of K.

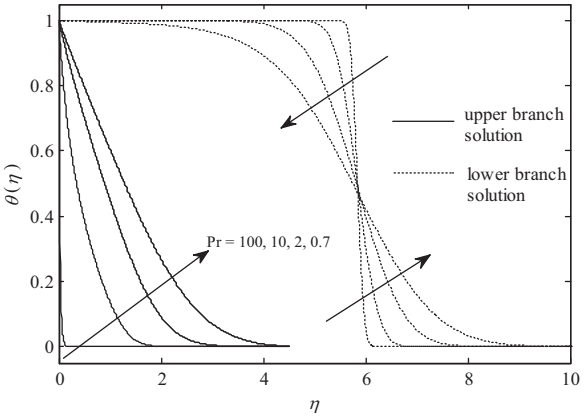

Fig. 4. Effect of Prandtl number Pr on the temperature profiles when $K = 0.1$, $\lambda = -1.2$, and $s = 0.5$.

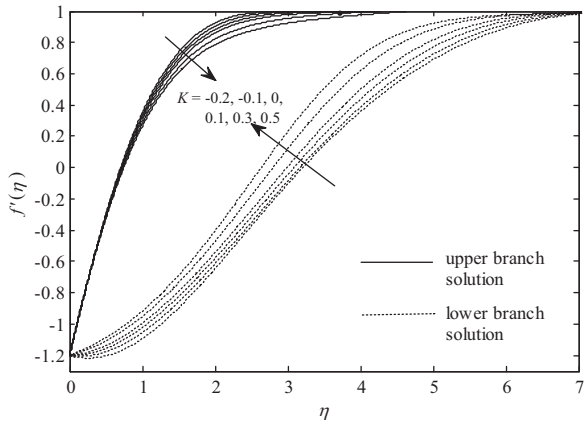

Fig. 5. Effect of elastic parameter K on the velocity profiles when $\lambda = -1.2$ and $s = 0.5$.

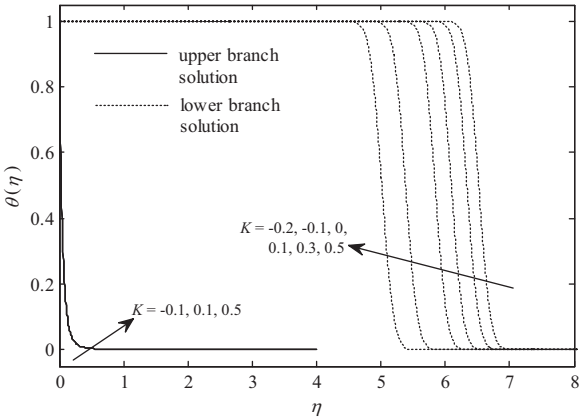

Fig. 6. Effect of elastic parameter K on the temperature profiles when $\lambda = -1.2$, $s = 0.5$, and $\Pr = 50$.

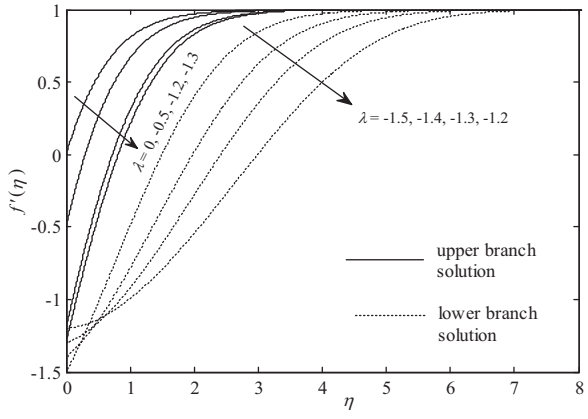

Fig. 7. Effect of shrinking parameter λ on the velocity profiles when $K = 0.1$ and $s = 0.5$.

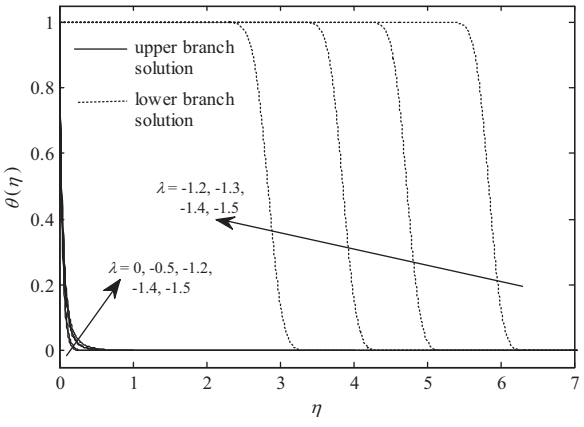

Fig. 8. Effect of shrinking parameter λ on the temperature profiles when $K = 0.1$, $s = 0.5$, and $\Pr = 50$.

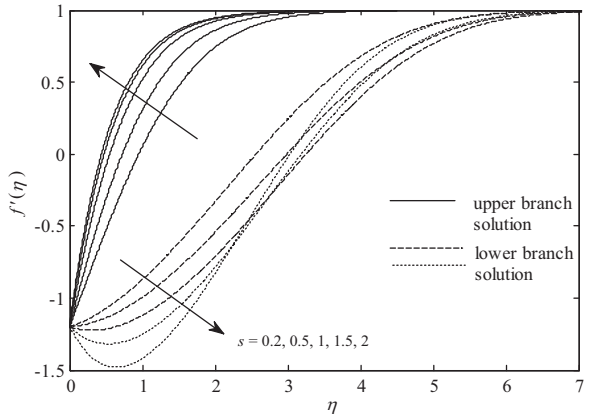

Fig. 9. Effect of suction parameter s on the velocity profiles when $K = 0.1$ and $\lambda = -1.2$.

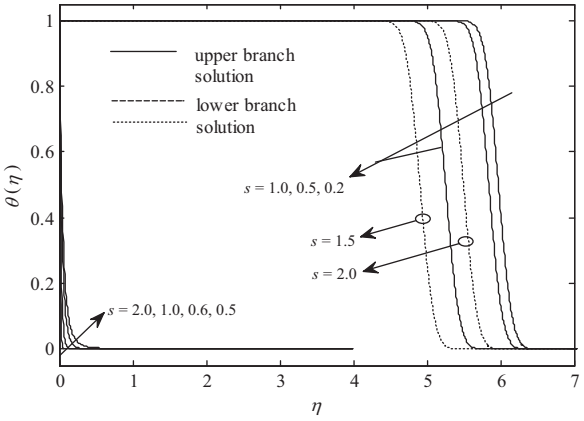

Fig. 10. Effect of suction parameter s on the temperature profiles when $K = 0.1$, $\lambda = -1.2$, and $\mathrm{Pr} = 50$.

model (velocity overshoot) considered by Beard and Walters [8].

In order to investigate the effect of governing parameters on the flow and heat transfer characteristics of the present problem, the variations of $f''(0)$ and reduced heat flux from the surface of the sheet $-\theta'(0)$ with the change in the shrinking parameter λ are given in Figures 2 and 3, respectively. It is observed that for fixed Prandtl number ($\mathrm{Pr} = 0.7$) and suction parameter ($s = 0.5$), both $f''(0)$ and $-\theta'(0)$ decreases as elastic parameter K increases. Figures 2 and 3 also show that a unique solution is found for $\lambda \geq -1$. Meanwhile, the existence of dual solutions for the shrinking sheet case is found when $\lambda_c < \lambda < -1$, where the critical values of λ are $\lambda_c \approx -1.512$, -1.498, and -1.482 for $K = 0.1$, 0.3, and 0.5, respectively.

Figure 4 shows the effect of Prandtl number on the dimensionless temperature profiles $\theta(\eta)$ when $K = 0.1$, $\lambda = -1.2$, and $s = 0.5$. These profiles are presented for $\mathrm{Pr} = 0.7$, 2, 10, and 100. The profiles for $\mathrm{Pr} > 100$ are too close to the one of $\mathrm{Pr} = 100$, therefore there are not plotted in Figure 4. It has to be mentioned here that it is difficult for us to obtain a converged solution for very large Pr, we believed that another approach need to be used for finding an asymptotic limit of large values of Pr.

Figures 5 – 10 present the velocity $f'(\eta)$ and temperature $\theta(\eta)$ profiles obtained for the UCM fluid near

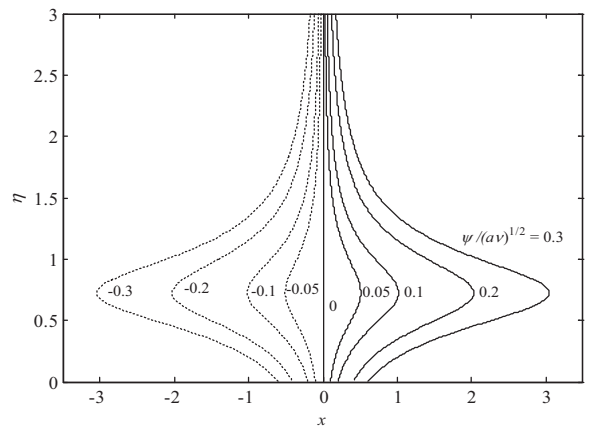

Fig. 11. Streamlines for upper branch solutions when $K = 0.1$, $\lambda = -1.2$, and $s = 0.5$.

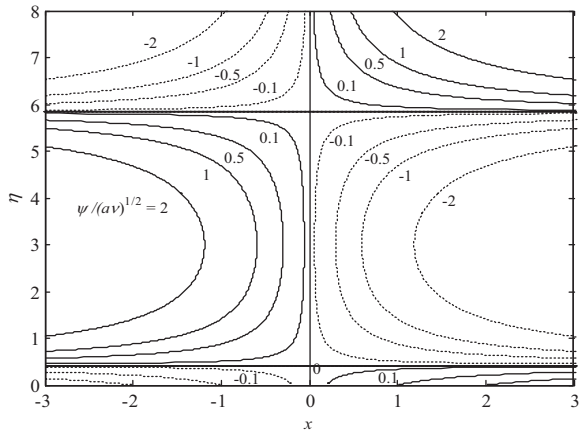

Fig. 12. Streamlines for lower branch solutions when $K = 0.1$, $\lambda = -1.2$, and $s = 0.5$.

a stagnation-point flow with the combination effects of elastic, shrinking, and suction parameters. The profiles are plotted for $\Pr = 50$ and different values of K, λ, and s. From the upper branch solutions in Figures 5 and 6, the velocity $f'(\eta)$ is found to decrease while the temperature $\theta(\eta)$ is found to increases with increasing K. An opposite trend is found for both profiles for the lower branch solutions. On the other hand, the momentum boundary layer thickness increases as the fluid elasticity increases; this is in agreement with the findings by Sadeghy et al. [6] and Kumari and Nath [7]. The increase in thermal boundary layer thickness in Figure 6 is not significant by an increase in the values of K. From the physical point of view, increase in elastic parameter will increase the resistance of fluid motion, which means the velocity will decrease and the momentum boundary layer thickness will increase as K increases.

The velocity profile $f'(\eta)$ in Figure 7 shows that the momentum boundary layer thickness decreases as $|\lambda|$ increases, but the thermal boundary layer thickness presented in Figure 8 shows the opposite trend. The effects of suction parameter s on the velocity and temperature profiles when $K = 0.1$, $\lambda = -1.2$, and $\Pr = 50$ are presented in Figures 9 and 10. Non-unique solutions are obtained for suction ($s > 0$). For the upper branch solution, the velocity gradient increases as s increases. However, for the lower branch solution, a negative velocity gradient is observed (back flow) near the shrinking sheet and then gradually change to positive as the distance from the sheet increases. Physically, the positive velocity gradient implies that the fluid exerts a drag forces on the wall surface and a negative sign implies the opposite.

Figures 11 and 12 show the symmetric stagnation flow towards a shrinking sheet ($\lambda = -1.2$) with suction ($s = 0.5$) for the upper branch and the lower branch solutions, respectively, where the dimensionless stream function $\bar{\psi}$ is defined as $\bar{\psi} = \psi/(a\upsilon)^{1/2}$. Because of the shrinking effect, the flow is dragged to the origin of the sheet whereas the effect of suction is obvious in Figure 11 where the flow is pulled to the permeable sheet. For the lower branch solution in Figure 12, the streamlines are divided into three regions. The first upper region shows that the oncoming flows pass on both sides, and the pattern is similar to normal stagnation-point flow. In the second region, reverse rotating flow is formed while in the lowest region, the flows are sucked to the permeable sheet. However, the effect of shrinking to the lower branch solutions is not obvious since the flow is not dragged significantly to the origin of the sheet.

It is worth mentioning to this end that we define the first solution as upper branch solution for which the value of $f''(0)$ is greatest (Riley and Weidman [30]) while the second solution is defined as lower branch solution. The stability analysis of the dual solutions of several boundary layer problems has been made by Merkin [31], Weidman et al. [32], Harris et al. [33], Postelnicu and Pop [34], and Roşca and Pop [35]. They revealed that the solutions along the upper branch (first) solution are linearly stable and physically realizable, whilst those on the lower branch (second) solution are linearly unstable and, therefore, physically not realizable. Therefore, we postulate that this conclusion is applicable also for the present problem. The stability analysis of the present problem is out of the scope of this paper.

5. Conclusions

The problem of stagnation-point flow and heat transfer towards a permeable shrinking sheet which obeys the UCM model was studied numerically. A similarity transformation was employed to reduce the governing partial differential equations into a system of ordinary differential equations, before being solved numerically by the Keller-box method. The effects of the governing parameters, namely elastic parameter K, shrinking parameter λ, and suction parameter s on the flow and heat transfer characteristics were thoroughly examined and discussed for some values of Prandtl number. Dual solutions were obtained for some values of the shrinking and suction parameters. Furthermore, it was found that the range of K for which the solution exists decreases with increasing K. The streamline pattern of the upper branch solutions are simpler and controllable compared to the streamline pattern of the lower branch solutions.

Acknowledgements

The first author would like to acknowledge the financial support received from the Universiti Sains Malaysia (USM) under a short term Grant No. 304/PJJAUH/6310099. The authors wish to express their thanks to the reviewers for the valuable comments and suggestions.

[1] N. Phan-Thien, Rheol. Acta **22**, 127 (1983).
[2] T. Hayat, Z. Abbas, and M. Sajid, Chaos Solit. Fract. **39**, 840 (2009).
[3] Z. Abbas, Y. Wang, T. Hayat, and M. Oberlack, Nonlin. Anal.: Real World Appl. **11**, 3218 (2010).
[4] T. Hayat, M. Mustafa, S. A. Shehzad, and S. Obaidat, Int. J. Numer. Methods Fluids **68**, 233 (2012).
[5] S. Nadeem, N. Akbar, A. Yıldırım, A. Hussain, and M. Ali, Compos. Mech. Comput. Appl. **2**, 297 (2011).
[6] K. Sadeghy, H. Hajibeygi, and S. M. Taghavi, Int. J. Non-Lin. Mech. **41**, 1242 (2006).
[7] M. Kumari and G. Nath, Int. J. Non-Lin. Mech. **44**, 1048 (2009).
[8] D. W. Beard and K. Walters, Math. Proc. Cambridge Philos. Soc. **60**, 667 (1964).
[9] J. E. Dunn and K. R. Rajagopal, Int. J. Eng. Sci. **33**, 689 (1995).
[10] V. K. Garg and K. R. Rajagopal, Mech. Res. Commun. **17**, 415 (1990).
[11] K. R. Rajagopal, Int. J. Non-Lin. Mech. **47**, 72 (2012).
[12] C. Y. Wang, Quart. Appl. Math. **48**, 601 (1990).
[13] M. Miklavčič and C. Y. Wang, Quart. Appl. Math. **64**, 283 (2006).
[14] C. Y. Wang, Int. J. Non-Lin. Mech. **43**, 377 (2008).
[15] P. Saikrishnan and S. Roy, Int. J. Eng. Sci. **41**, 1351 (2003).
[16] S. Roy and P. Saikrishnan, Int. J. Heat Mass Tran. **46**, 3389 (2003).
[17] S. Mukhopadhyay and G. C. Layek, Int. J. Heat Mass Tran. **51**, 2167 (2008).
[18] M. S. Shadloo and A. Kimiaeifar, J. Mech. Eng. Sci. **225**, 347 (2011).
[19] M. S. Shadloo, A. Kimiaeifar, and D. Bagheri, Int. J. Numer. Meth. Heat Fluid Flow **23**, 289 (2013).
[20] K. Sadeghy, A.-H. Najafi, and M. Saffaripour, Int. J. Non-Lin. Mech. **40**, 1220 (2005).
[21] B. Sakiadis, AIChE J **7**, 221 (1961).
[22] R. B. Bird, R. C. Armstrong, and O. Hassager, Dynamics of Polymeric Liquids (2nd ed.), Wiley, New York 1987.
[23] K. Hiemenz, Dingler's Polytech. J. **326**, 321 (1911).
[24] T. Cebeci and P. Bradshaw, Physical and Computational Aspects of Convective Heat Transfer, Springer, New York 1988.
[25] T Cebeci, Convective Heat Transfer (2nd revised ed.), Horizons Publishing, California 2002.
[26] Y. Y. Lok, N. Amin, and I. Pop, Int. J. Heat Mass Trans. **50**, 4855 (2007).
[27] A. Ishak, R. Nazar, and I. Pop, Comput. Math. Appl. **56**, 3188 (2008).
[28] A. Ishak, Y. Y. Lok, and I. Pop, Chem. Eng. Commun. **197**, 1417 (2010).
[29] A. Kimiaeifar, G. H. Bagheri, M. Rahimpour, and M. A. Mehrabian, J. Proc. Mech. Eng. **223**, 133 (2009).
[30] N. Riley and P. D. Weidman, SIAM J. Appl. Math. **49**, 1350 (1989).
[31] J. H. Merkin, J. Eng. Math. **20**, 171 (1985).
[32] P. D. Weidman, D. G. Kubitschek, and A. M. J. Davis, Int. J. Eng. Sci. **44**, 730 (2006).
[33] D. Harris, D. B. Ingham, and I. Pop, Transp. Porous Media **77**, 267 (2009).
[34] A. Postelnicu and I. Pop, Appl. Math. Comput. **217**, 4359 (2011).
[35] A. V. Roşca and I. Pop, Int. J. Heat Mass Trans. **60**, 355 (2013).